

Passive Geolocation with Unmanned Aerial Vehicles using AOA Measurement Processing

Grigoriy Fokin*

* *State University of Telecommunication, 22 Prospekt Bolshevikov, St. Petersburg, Russia*
grihafokin@gmail.com

Abstract—This paper considers 3 dimensional (3D) angle of arrival (AOA) measurements processing model for positioning a transmitter by cooperation of flying segment based on receiver station aboard Unmanned Aerial Vehicle (UAV) with terrestrial segment including stationary ground receiver station and confirms its practicability for handling Non-Line-Of-Sight (NLOS) problem. Positioning with UAVs is especially relevant in heterogeneous terrain with inherent reflections resulting in primary measurements distortion. NLOS problem was well investigated for 2D scenarios with ground receiver stations, however for 3D UAV based positioning this is a topic of ongoing research. In this paper different measurement processing techniques and results for UAV based location were analyzed to explore advantages and shortcomings of AOA among others. The contribution of the current research is the refinement of mathematical and simulation models for positioning of radio transmitter with one stationary ground and one flying UAV based receiver station using AOA processing and its performance evaluation with handling AOA noise. Resulting estimates agree with known results for UAV based positioning and validate its practicability to face NLOS problem, when AOA deviation is less than 10 degrees.

Keyword — Cramer-Rao bounds, Direction-of-arrival estimation, Position measurement, Radar signal processing, Root mean square, Unmanned aerial vehicles

I. INTRODUCTION

THIS work presents geolocation application of actual wireless networks which widely exploit joint cooperation of flying segment based on transceiver stations aboard Unmanned Aerial Vehicles (UAVs) with terrestrial segment including stationary ground transceiver stations [1]. Geolocation tasks in such networks are essential for both military applications, for example, in tactical networks [3] or battlefield environments [4], and civil applications, for instance, in ground-aerial surveillance [5], search and rescue operations [6], drone-equipped wireless control measurement [2] and flying sensor networks [1].

Positioning is implemented from passive measurements of

the arrival times, directions of arrival, or Doppler shifts of electromagnetic waves received at various sites [7].

UAV based positioning techniques had already got considerable attention in the past years and can be subdivided by primary measurements into Time Difference of Arrival (TDOA) [9]–[14], Frequency Difference of Arrival (FDOA) [15], Angle of Arrival (AOA) [16], [17] and Received Signal Strength Indication (RSSI) [18], [19] positioning.

Every measurement processing technique based on TDOA, FDOA, AOA or RSSI has its advantages and shortcomings. While TDOA technique could achieve high accuracy in optimistic Line of Sight (LOS) conditions, it requires precise receiver synchronization. In 3D at least four receivers are required for TDOA. On the other hand, DOA technique requires less number of receivers and neither synchronization among them, however it needs an antenna array for each receiver and resulting location accuracy is highly dependent on the distance between the object of location and receivers. RSSI based localization is preferred in many applications because of the simple implementation, but its accuracy degrades in large scale environments [8] due to inherent variation of the received signal strength (RSS).

The use of UAVs as moving receiver in conjunction with stationary ground based receiver, reducing the number of sensors required to obtain multiple TDOA measurements, was presented in [9], [10]. Recursive location estimation of a stationary and moving transmitter from a pair of UAVs using TDOA was investigated for Kalman [11] and Gaussian [12] filtering techniques. Cooperation of flying segment based on receiver station aboard UAV with terrestrial segment including several stationary ground receivers using TDOA was investigated in [13], [14] and achieved accuracy of 10 m. Mobile emitter geolocation and tracking using TDOA and FDOA fusion is considered in [15].

Hierarchical DOA estimation and the fusion of DOAs and the terrain map was proposed in [16] to reduce computational complexity of the near-real-time monitoring system. In [17] a series of both real-world flight testing and computer simulated scenarios were conducted to study the feasibility of a low-cost UAV DOA geolocation platform.

RSSI localization and tracking architecture, where a data driven neural network model is used for estimating unknown signal strength and extended Kalman filters are utilized for eliminating RSS noise is presented in [18]. Localization of a radio frequency (RF) transmitter with intermittent transmissions as quickly as possible via a group of UAVs with omnidirectional RSS sensors is considered in [19].

Observed accuracy results are summarized in Table 1.

Manuscript received December 29, 2018. This work was sponsored by the Ministry of Science and Education with Grant of the President of the Russian Federation for the state support of young Russian scientists № MK-3468.2018.9, and a follow-up of the invited journal to the accepted & presented paper of the XXIIth International Conference on Advanced Communication Technology (ICACT2019).

Grigoriy Fokin is with the Bonch-Bruевич Saint-Petersburg State University of Telecommunications (SUT), 22 Prospekt Bolshevikov, St. Petersburg, Russia (corresponding author phone: 8 921 985 80 04; e-mail: grihafokin@gmail.com).

TABLE I
ACCURACY RESULTS FOR UAV BASED POSITIONING

Ref.	Assumptions		Primary Measurements	
	Accuracy bounds, m	Layout		
[3]	21 – 100	3D, 1 UAV, LOS	TDOA	
[4]	16 – 99	3D, 1 UAV, LOS		
[9], [10]	500 – 2000	3D, 1 UAV, LOS		
[11]	10 – 1000	2D, 2 UAVs, LOS, Kalman filtering		
[12]	100 – 1000	2D, 2 UAVs, LOS, Kalman filtering		
[13], [14]	10 – 20	3D, 1 UAV, 5 Rx _{GR} , LOS		
[20]	20 – 5000	3D, 1 UAV, 5 Rx _{GR} , NLOS		
[21]	20 – 5000	2D, 5 Rx _{GR} , NLOS		
[15]	10 – 2000	2D, 2 UAVs, LOS, Kalman filtering		TDOA-FDOA
[16]	15 – 65	3D, 2 UAVs, LOS, terrain map		AOA
[17]	20 – 200	2D, 1 UAV, LOS		
[18]	28 – 57	3D, 3 UAVs, LOS, Kalman filtering	RSSI	
[19]	30 – 200	2D, 2 UAVs, LOS		

To validate AOA measurement processing for UAV based positioning in heterogeneous terrain with NLOS conditions let's analyze existing accuracy results for TDOA, FDOA, AOA techniques, shown in Table 1. Results are simulation based, differ noticeably and depend on a plenty of factors, including model setup and parameters. However, we can make following conclusions. Firstly, more receiver stations provide higher positioning accuracy. Secondly, transmitter location accuracy in 2D is mainly higher than in 3D scenarios. Thirdly, most results are valid for optimistic LOS conditions and do not account for possible reflections in heterogeneous terrain. However, positioning with UAVs is especially relevant in heterogeneous terrain, when primary NLOS measurements, obtained after reflections, could lead to a significant Root Mean Square Error (RMSE) exceeding 10^3 m [20], [21]. Thus, the task of current investigation is to refine existing AOA measurement processing technique for UAV based positioning model in [20], [21] and evaluate its robustness in handling AOA variance encountering primary measurements disturbances after NLOS reflections.

AOA measurement processing technique for positioning of transmitter was already investigated in [22], [23] and pointed that it is not able to directly apply existing 2D AOA models, because two angles have to be used jointly in their respective non-linear measurement equations in order to determine the position of the source, however, it did not take into account influence of moving receiver aboard UAV. Thus, it is reasonable to refine models in [20], [21] with 3D AOA measurement processing technique [22], [23] with joint azimuth and the elevation angle measurement equations.

The material in the paper is organized in the following order. Mathematical model for positioning of transmitter with one stationary ground and one flying UAV based receiver using AOA measurement processing is presented in Section II. Developed simulation model, scenario of positioning and numerical results for AOA positioning accuracy performance evaluation are given in Section III. Finally, we draw the conclusions in Section IV.

II. AOA MEASUREMENT PROCESSING IN UAV BASED POSITIONING

Here we present UAV based positioning model, AOA positioning geometry, measurement processing model and Cramer-Rao lower bound (CRLB) computation.

A. UAV Based Positioning Model

UAV based positioning system under consideration, including flying segment based on one receive sensor aboard UAV with terrestrial segment including one stationary ground receive sensor is shown in Figure 1.

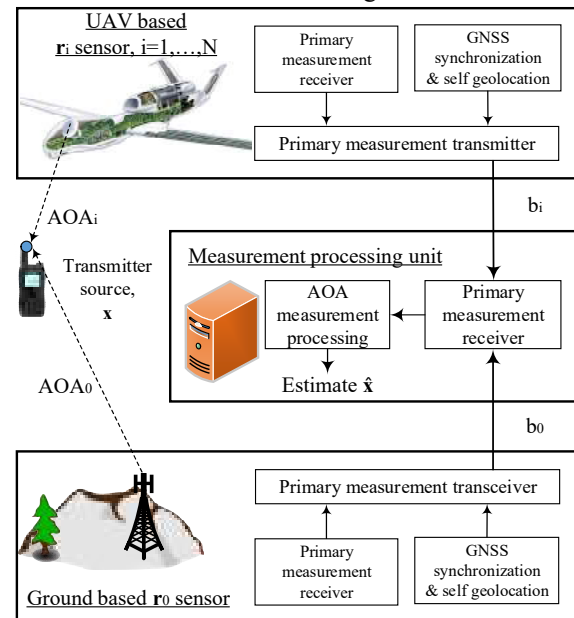


Fig. 1. UAV based positioning system.

Ground and UAV based receive sensors whose positions are available with Global Navigation Satellite Systems (GNSS) carry out the task of receiving primary AOA measurements from packets transmitted by radiating emitter source. Single passive sensor can record the time stamp and direction of the received packet. Accurate time stamping is possible since each sensors has a GNSS receiver for time synchronization. Then, AOAs of each sensor are forwarded to the measurement processing unit, which in turn using known sensor locations and AOA measurement processing estimate radiating emitter coordinates $\hat{\mathbf{x}} = [\hat{x}, \hat{y}, \hat{z}]$.

If positioning is carried out by AOA in three-dimensional space, flying UAV based receiver produces azimuth and elevation angles every time instant along UAV flight path as shown in Figure 2.

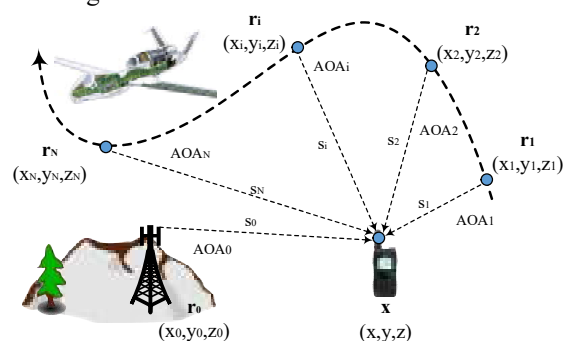


Fig. 2. Using of UAV as moving sensor with ground based sensor.

B. UAV Based AOA Positioning Geometry

Denote receive sensors with available coordinates $\mathbf{r}_i = [x_i, y_i, z_i]^T$, where time intervals $i = 0, \dots, N$ correspond to synchronized timestamps, N – the number of primary measurements along UAV flight path, and transmitter with unknown coordinates $\mathbf{x} = [x, y, z]^T$, then from Figure 3

$$\Delta x_i = x - x_i, \quad \Delta y_i = y - y_i, \quad \Delta z_i = z - z_i. \quad (1)$$

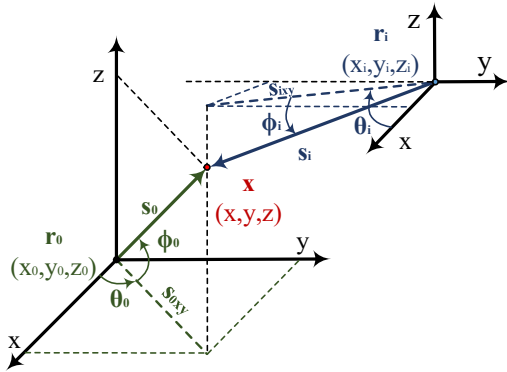


Fig. 3. Positioning geometry.

Relationship between \mathbf{x} and \mathbf{r}_i is given by [24]

$$\mathbf{x} = \mathbf{r}_i + \mathbf{s}_i, \quad (2)$$

where \mathbf{s}_i is the noise-free bearing vector connecting \mathbf{r}_i to \mathbf{x} .

Actual range between transmitter \mathbf{x} and sensor \mathbf{r}_i is defined as norm of bearing vector $\mathbf{s}_i = \mathbf{x} - \mathbf{r}_i$

$$s_i = \|\mathbf{s}_i\|_2 = \|\mathbf{x} - \mathbf{r}_i\|_2 = \sqrt{\Delta x_i^2 + \Delta y_i^2 + \Delta z_i^2}, \quad (3)$$

where $\|\cdot\|_2$ – norm operator over a vector [26]. Projection of bearing vector \mathbf{s}_i on x-y plane is defined by

$$s_{ixy} = \sqrt{\Delta x_i^2 + \Delta y_i^2}. \quad (4)$$

Actual error-free bearing pair including azimuth θ_i and elevation ϕ_i AOA from transmitter \mathbf{x} to sensor \mathbf{r}_i is

$$\theta_i = \arctg\left(\frac{\Delta y_i}{\Delta x_i}\right), \quad \phi_i = \arctg\left(\frac{\Delta z_i}{s_{ixy}}\right), \quad (5)$$

Using following notations from Figure 3

$$\cos \theta_i = \frac{\Delta x_i}{s_{ixy}}, \quad \sin \theta_i = \frac{\Delta y_i}{s_{ixy}}, \quad \cos \phi_i = \frac{s_{ixy}}{s_i}, \quad \sin \phi_i = \frac{\Delta z_i}{s_i}, \quad (6)$$

we can represent bearing vector \mathbf{s}_i as

$$\mathbf{s}_i = s_i [\cos \phi_i \cos \theta_i, \cos \phi_i \sin \theta_i, \sin \phi_i]^T. \quad (7)$$

C. AOA Measurement Processing Model

Relationship between azimuth angle θ_i and unknown transmitter coordinates can be derived using manipulation [25] for (5), yielding $\tan \theta_i = \Delta y_i / \Delta x_i$, or

$$\sin \theta_i \Delta x_i - \cos \theta_i \Delta y_i = 0. \quad (8)$$

Denote vector $\mathbf{a}_{2Di} = [\sin \theta_i, -\cos \theta_i, 0]^T$, then using notations in (1) we can rewrite (8) as

$$\mathbf{a}_{2Di}^T \mathbf{x} = \mathbf{a}_{2Di}^T \mathbf{r}_i, \quad (9)$$

where \mathbf{a}_{2Di} satisfies $\mathbf{a}_{2Di}^T \mathbf{s}_i = 0$ and $\|\mathbf{a}_{2Di}\|_2 = 1$ as in [24].

Expressions (5) represent error-free values of AOA, noisy measured AOA can be rewritten as

$$\tilde{\theta}_i = \theta_i + n_{\theta_i}, \quad \tilde{\phi}_i = \phi_i + n_{\phi_i}, \quad (10)$$

where n_{θ_i} and n_{ϕ_i} are white Gaussian with zero mean with variables $\sigma_{\theta_i}^2$ and $\sigma_{\phi_i}^2$, respectively. Then (9) can be rewritten

$$\tilde{\mathbf{a}}_{2Di}^T \mathbf{x} = \tilde{\mathbf{a}}_{2Di}^T \mathbf{r}_i + n_{2Di}, \quad (11)$$

where $\tilde{\mathbf{a}}_{2Di} = [\sin \tilde{\theta}_i, -\cos \tilde{\theta}_i, 0]^T$ and term $n_{2Di} = \tilde{\mathbf{a}}_{2Di}^T \mathbf{s}_i$.

Relationship between elevation angle ϕ_i and unknown transmitter coordinates can be derived using manipulation [25] for (5), yielding $\tan \phi_i = \Delta z_i / s_{ixy}$, or

$$\sin \phi_i s_{ixy} - \cos \phi_i \Delta z_i = 0. \quad (12)$$

Expressing s_{ixy} in (4) with notations in (6) yields

$$s_{ixy} = \Delta x_i \Delta x_i / \sqrt{\Delta x_i^2 + \Delta y_i^2} + \Delta y_i \Delta y_i / \sqrt{\Delta x_i^2 + \Delta y_i^2} = \Delta x_i \cos \theta_i + \Delta y_i \sin \theta_i, \quad (13)$$

and putting (13) in (12) we get

$$\Delta x_i \sin \phi_i \cos \theta_i + \Delta y_i \sin \phi_i \sin \theta_i - \Delta z_i \cos \phi_i = 0. \quad (14)$$

Denote vector $\mathbf{a}_{3Di} = [\sin \phi_i \cos \theta_i, \sin \phi_i \sin \theta_i, -\cos \phi_i]^T$, then using notations in (4) we can rewrite (14) as

$$\mathbf{a}_{3Di}^T \mathbf{x} = \mathbf{a}_{3Di}^T \mathbf{r}_i, \quad (15)$$

where \mathbf{a}_{3Di} satisfies $\mathbf{a}_{3Di}^T \mathbf{s}_i = 0$ and $\|\mathbf{a}_{3Di}\|_2 = 1$ as in [24].

Using noisy measured AOA, (15) can be rewritten [25]

$$\tilde{\mathbf{a}}_{3Di}^T \mathbf{x} = \tilde{\mathbf{a}}_{3Di}^T \mathbf{r}_i + n_{3Di}, \quad (16)$$

with $\tilde{\mathbf{a}}_{3Di} = [\sin \tilde{\phi}_i \cos \tilde{\theta}_i, \sin \tilde{\phi}_i \sin \tilde{\theta}_i, -\cos \tilde{\phi}_i]^T$, $n_{3Di} = \tilde{\mathbf{a}}_{3Di}^T \mathbf{s}_i$.

Concatenating (11) and (16) gives following system

$$\mathbf{A} \mathbf{x} = \mathbf{r} + \mathbf{n}, \quad (17)$$

where $\mathbf{A} \in \mathbb{R}^{2(N+1) \times 3}$, $\mathbf{r} \in \mathbb{R}^{2(N+1) \times 1}$, $\mathbf{n} \in \mathbb{R}^{2(N+1) \times 1}$:

$$\mathbf{A} = \begin{bmatrix} \tilde{\mathbf{a}}_{2D0}^T \\ \vdots \\ \tilde{\mathbf{a}}_{2DN}^T \\ \tilde{\mathbf{a}}_{3D0}^T \\ \vdots \\ \tilde{\mathbf{a}}_{3DN}^T \end{bmatrix}, \quad \mathbf{r} = \begin{bmatrix} \tilde{\mathbf{a}}_{2D0}^T \mathbf{r}_0 \\ \vdots \\ \tilde{\mathbf{a}}_{2DN}^T \mathbf{r}_N \\ \tilde{\mathbf{a}}_{3D0}^T \mathbf{r}_0 \\ \vdots \\ \tilde{\mathbf{a}}_{3DN}^T \mathbf{r}_N \end{bmatrix}, \quad \mathbf{n} = \begin{bmatrix} n_{2D0} \\ \vdots \\ n_{2DN} \\ n_{3D0} \\ \vdots \\ n_{3DN} \end{bmatrix}. \quad (18)$$

D. CRLB for AOA Measurement Processing Model

Bearing pair $\mathbf{b}_i \in \mathbb{R}^{2 \times 1}$ with θ_i and ϕ_i is represented by $\mathbf{b}_i = [\theta_i, \phi_i]^T$, after N timestamps forms array $\mathbf{B} \in \mathbb{R}^{2(N+1) \times 1}$, defined by $\mathbf{B}(\mathbf{x}) = [\theta_0, \dots, \theta_N, \phi_0, \dots, \phi_N]^T$. Jacobian matrix $\mathbf{J}(\mathbf{x}) = \partial \mathbf{B}(\mathbf{x}) / \partial \mathbf{x} \in \mathbb{R}^{2(N+1) \times 3}$ can be computed as

$$\mathbf{J}(\mathbf{x}) = \begin{bmatrix} -\frac{\sin \theta_0}{s_{0xy}} & \frac{\cos \theta_0}{s_{0xy}} & 0 \\ s_{0xy} & s_{0xy} & \vdots \\ \vdots & \vdots & \vdots \\ -\frac{\sin \theta_N}{s_{Nxy}} & \frac{\cos \theta_N}{s_{Nxy}} & 0 \\ s_{Nxy} & s_{Nxy} & \vdots \\ \cos \theta_0 \sin \phi_0 & -\sin \theta_0 \sin \phi_0 & \cos \phi_0 \\ s_0 & s_0 & s_0 \\ \vdots & \vdots & \vdots \\ -\cos \theta_N \sin \phi_N & \sin \theta_N \sin \phi_N & \cos \phi_N \\ s_N & s_N & s_N \end{bmatrix} \cdot (19)$$

The key in producing the CRLB is to construct the corresponding Fisher information matrix (FIM), computed at transmitter location $\mathbf{x} = [x, y, z]^T$. The diagonal elements of the FIM inverse are the minimum achievable variance values:

$$\text{CRLB}(\mathbf{x}) = \text{trace}(\text{FIM}^{-1}(\mathbf{x})). \quad (20)$$

When the primary AOA measurements are zero-mean Gaussian distributed, FIM(\mathbf{x}) can be computed as [26]

$$\text{FIM}(\mathbf{x}) = \mathbf{J}^T(\mathbf{x}) \mathbf{C}^{-1} \mathbf{J}(\mathbf{x}), \quad (21)$$

where $\mathbf{C} \in \mathbb{R}^{2(N+1) \times 2(N+1)}$ is AOA noise covariance matrix

$$\mathbf{C} = \sigma_{\text{AOA}} \mathbf{I}, \quad (22)$$

where σ_{AOA} is AOA standard deviation for azimuth σ_{θ_i} and elevation σ_{ϕ_i} , and $\mathbf{I} \in \mathbb{R}^{2(N+1) \times 2(N+1)}$ is identity matrix.

Numerical search to solve (17) was the Gauss-Newton least squares (LS) algorithm which solves for \mathbf{x} by minimizing the LS cost function

$$\hat{\mathbf{x}} = \arg \min_{\mathbf{x}} (\tilde{\mathbf{B}} - \mathbf{B}(\mathbf{x}))^T (\tilde{\mathbf{B}} - \mathbf{B}(\mathbf{x})), \quad (23)$$

where $\tilde{\mathbf{B}} = [\tilde{\theta}_0, \dots, \tilde{\theta}_N, \tilde{\phi}_0, \dots, \tilde{\phi}_N]^T$ is bearing measurement array. The iterative GN algorithm procedure is

$$\hat{\mathbf{x}}_{k+1} = \hat{\mathbf{x}}_k + \mathbf{J}^T(\hat{\mathbf{x}}_k) \mathbf{J}(\hat{\mathbf{x}}_k)^{-1} (\tilde{\mathbf{B}} - \mathbf{B}(\hat{\mathbf{x}}_k)), \quad (24)$$

where $\mathbf{J}(\hat{\mathbf{x}}_k)$ is Jacobian matrix (19) computed at $\hat{\mathbf{x}}_k$. Initial value for the iterative GN algorithm (24) is calculated as the mean of the receiver positions \mathbf{r}_i along UAV flight path.

The RMSE of coordinates estimate of transmitter is [27]

$$\text{RMSE} = \sqrt{E \left\{ \sqrt{(x - \hat{x})^2 + (y - \hat{y})^2 + (z - \hat{z})^2} \right\}}. \quad (25)$$

where $\hat{\mathbf{x}} = [\hat{x}, \hat{y}, \hat{z}]$ is transmitter GN location estimate.

III. SIMULATION SCENARIO AND RESULTS

Simulation model described further include arrangement, estimation and visualization subsystems, described in [20], [21]. Positioning was performed for scenario when transmitter is at the point (5, 4, 1) km in an area with a size of (10 × 10 × 5) km, stationary ground receiver is at the origin point (0, 0, 0) km, and UAV flies circumferentially over the area at a constant altitude $z = 4$ km, as depicted in Figure 4.

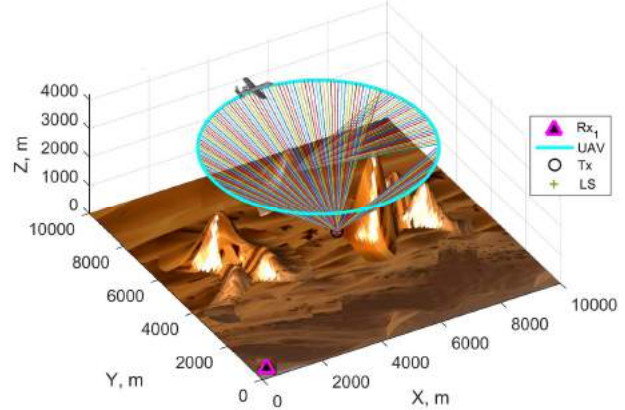


Fig. 4. Example NLOS simulation scenario with ground and UAV receiver.

In Figure 4 we have illustrated scenario when moving receiver aboard UAV produces NLOS measurements because of mountain obstacle for a short time flight. Resulting RMSE of current estimates in three axes according to UAV flight is provided in Figure 5.

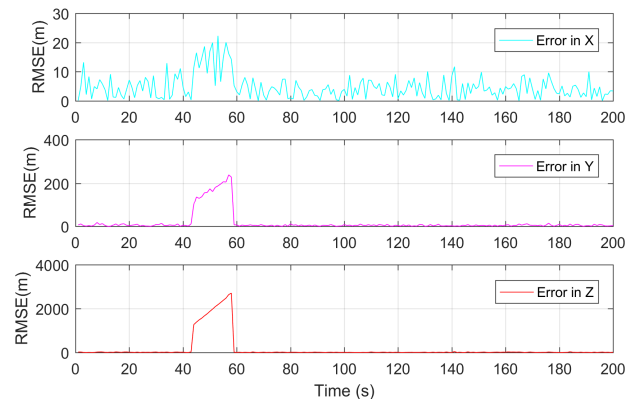


Fig. 5. RMSE estimation for scenario in Fig 4.

From Figure 5 it can be seen that the RMSE considerably increases in the interval from 42 s to 60 s, which is illustrated by reflected rays, when LOS between UAV and transmitter is absent and NLOS measurement comes after reflection from mountain during the UAV flight behind the obstacle.

Figure 6 shows resulting location RMSE versus AOA standard deviation σ_{AOA} for azimuth $\sigma_{\theta_i}^2$ and elevation $\sigma_{\phi_i}^2$ angles, and it can be seen, that RMSE quickly degrades with the increase of AOA noise and reaches the order of 10^3 m, when AOA deviation σ_{AOA} approaches 10 degrees.

RMSE order of 10^3 m is considerably higher, than LOS [13], [14], but lower, than NLOS transmitter location error [20], [21]. Approach to identify and exclude NLOS error, validated in [20], [21], utilizes RMSE threshold, which should be higher than LOS error for worst SNR values and, at the same time, lower than location error for NLOS scenario.

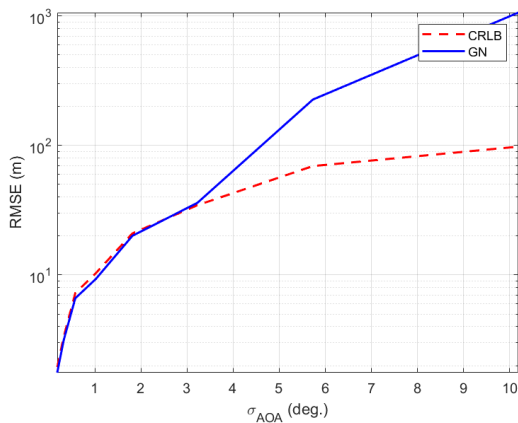


Fig. 6. Emitter location RMSE versus AOA standard deviation σ_{AOA} .

IV. CONCLUSION

In this paper we refined 3D AOA measurements processing model for positioning a transmitter with one stationary ground and one flying UAV based receiver station. Performed simulation results validate possibility to handle NLOS with just two stations, because even coarse AOA with $\sigma_{AOA} < 10^\circ$ can contribute to NLOS measurements identifying.

REFERENCES

- [1] V. A. Mochalov and A. P. Pschenichnikov, "Functional scheme of the flying sensor networks architecture design," *2016 18th International Conference on Advanced Communication Technology (ICACT)*, Pyeongchang, 2016, pp. 659-663.
- [2] Y. Lee, Y. Lee, Y. Jang and M. Park, "A process-aware drone-equipped 3D engine and wireless control measurement platform for integrated management of SOC facilities," *2018 20th International Conference on Advanced Communication Technology (ICACT)*, Chuncheon, Gangwondo, Korea (South), 2018, pp. 1067-1072.
- [3] O. D. Saputra, M. Irfan, N. N. Putri and S. Y. Shin, "UAV-based localization for distributed tactical wireless networks using archimedean spiral," *2015 International Symposium on Intelligent Signal Processing and Communication Systems (ISPACS)*, Nusa Dua, 2015, pp. 392-396.
- [4] D. Kim, K. Lee, M. Park and J. Lim, "UAV-Based Localization Scheme for Battlefield Environments," *MILCOM 2013 - 2013 IEEE Military Communications Conference*, San Diego, CA, 2013, pp. 562-567.
- [5] G. Stamatescu, D. Popescu and R. Dobrescu, "Cognitive radio as solution for ground-aerial surveillance through WSN and UAV infrastructure," *Proceedings of the 2014 6th International Conference on Electronics, Computers and Artificial Intelligence (ECAI)*, Bucharest, 2014, pp. 51-56.
- [6] S. Waharte and N. Trigoni, "Supporting Search and Rescue Operations with UAVs," *2010 International Conference on Emerging Security Technologies*, Canterbury, 2010, pp. 142-147.
- [7] D. J. Torrieri, "Statistical Theory of Passive Location Systems," in *IEEE Transactions on Aerospace and Electronic Systems*, vol. AES-20, no. 2, pp. 183-198, March 1984.
- [8] M. Sivers, G. Fokin, P. Dmitriev, A. Kireev., D. Volgushev, A. Ali, "Indoor Positioning in WiFi and NanoLOC Networks," *Lecture Notes in Computer Science*, vol. 9870, pp. 465-476, 2016.
- [9] H.-J. Du and P. Y. Lee, "Passive Geolocation Using TDOA Method from UAVs and Ship/Land-Based Platforms for Maritime and Littoral Area Surveillance," Defense R and D, Ottawa, Canada, Technical Memorandum 2004-033, Feb. 2004.
- [10] H.-J. Du and P. Y. Lee, "Simulation of multi-platform geolocation using a hybrid TDOA-AOA method," Defense R and D Ottawa, Canada, Technical Memorandum 2004-256, Dec. 2004.
- [11] F. Fletcher, Branko Ristic and Darko Musicki, "Recursive estimation of emitter location using TDOA measurements from two UAVs," *2007 10th International Conference on Information Fusion*, Quebec, Que., 2007, pp. 1-8.
- [12] N. Okello, F. Fletcher, D. Musicki and B. Ristic, "Comparison of Recursive Algorithms for Emitter Localisation using TDOA Measurements from a Pair of UAVs," in *IEEE Transactions on Aerospace and Electronic Systems*, vol. 47, no. 3, pp. 1723-1732, July 2011.
- [13] A. H. A. Al-odhari, G. Fokin and A. Kireev, "Positioning of the radio source based on time difference of arrival method using unmanned aerial vehicles," *2018 Systems of Signals Generating and Processing in the Field of on Board Communications*, Moscow, 2018, pp. 1-5.
- [14] Fokin, G. A., Alodhari, A. H., "TDOA measurement processing for positioning using unmanned aerial vehicles," *T-Comm (Media Publisher)*, vol. 12, № 7, pp. 52-58, 2018.
- [15] D. Musicki, R. Kaune and W. Koch, "Mobile Emitter Geolocation and Tracking Using TDOA and FDOA Measurements," in *IEEE Transactions on Signal Processing*, vol. 58, no. 3, pp. 1863-1874, March 2010.
- [16] Z. Wang, E. Blasch, G. Chen, D. Shen, X. Lin and K. Pham, "A low-cost, near-real-time two-UAS-based UWB emitter monitoring system," in *IEEE Aerospace and Electronic Systems Magazine*, vol. 30, no. 11, pp. 4-11, November 2015.
- [17] M. A. Magers, "Geolocation of RF Emitters Using a Low-Cost UAV-Based Approach," M. Sci. thesis, Air Force Institute of Technology, Write-Patterson Air Force Base, Ohio, United States, 2016.
- [18] M. Hasanzade, O. Herekoglul, N. K. Ure, E. Koyuncu, R. Yeniceri and G. Inalhan, "Localization and tracking of RF emitting targets with multiple unmanned aerial vehicles in large scale environments with uncertain transmitter power," *2017 International Conference on Unmanned Aircraft Systems (ICUAS)*, Miami, FL, USA, 2017, pp. 1058-1065.
- [19] F. Koohifar, I. Guvenc and M. L. Sichitiu, "Autonomous Tracking of Intermittent RF Source Using a UAV Swarm," in *IEEE Access*, vol. 6, pp. 15884-15897, 2018.
- [20] Fokin G., Ali A.A.H., "Algorithm for Positioning in Non-line-of-Sight Conditions Using Unmanned Aerial Vehicles," *Lecture Notes in Computer Science*, vol. 11118, pp. 496-508, 2018.
- [21] G. Fokin, "TDOA Measurement Processing for Positioning in Non-Line-of-Sight Conditions," *2018 IEEE International Black Sea Conference on Communications and Networking (BlackSeaCom)*, Batumi, 2018, pp. 1-5.
- [22] Y. Wang and K. C. Ho, "An Asymptotically Efficient Estimator in Closed-Form for 3-D AOA Localization Using a Sensor Network," in *IEEE Transactions on Wireless Communications*, vol. 14, no. 12, pp. 6524-6535, Dec. 2015.
- [23] J. Yin, Q. Wan, S. Yang and K. C. Ho, "A Simple and Accurate TDOA-AOA Localization Method Using Two Stations," in *IEEE Signal Processing Letters*, vol. 23, no. 1, pp. 144-148, Jan. 2016.
- [24] K. Dogancay and G. Ibal, "Instrumental Variable Estimator for 3D Bearings-Only Emitter Localization," *2005 International Conference on Intelligent Sensors, Sensor Networks and Information Processing*, Melbourne, Australia, 2005, pp. 63-68.
- [25] L. Badrials, H. Kennedy and A. Finn, "Effects of coordinate system rotation on two novel closed-form localization estimators using azimuth/elevation," *Proceedings of the 16th International Conference on Information Fusion*, Istanbul, 2013, pp. 1797-1804.
- [26] R. Zekavat, R. M. Buehrer, *Handbook of position location: Theory practice and advances*, Wiley-IEEE Press, 2011.
- [27] G. Mashkov, E. Borisov and G. Fokin, "Experimental validation of multipoint joint processing of range measurements via software-defined radio testbed," *2017 19th International Conference on Advanced Communication Technology (ICACT)*, Bongpyeong, 2017, pp. 979-984.



Ph. D. Grogoryi Fokin (M'18) is with the Bonch-Bruевич Saint-Petersburg State University of Telecommunications (SUT) as Associate Professor of the Department of Radio Communications and became a Member (M) of IEEE in 2018.

He graduated SUT in 2005, then received Ph. D there in 2009 and from 2010 till 2014 worked as Senior Researcher in Radio Research and Development Institute (NIIR).

Mr. Fokin is author of 61 scientific papers, 5 tutorials and winner of grant competition of the President of the Russian Federation for the state support of young Russian scientists № MK-3468.2018.9.